Supporting Information

Marriott *et al.* 10.1073/pnas.0808882105

SI Text

Synthesis of C11-NitroBIPS. C11-NitroBIPS was prepared according to the methods described in Sakata *et al.* (1). Briefly, 2,3,3-trimethyl-3H-indole was refluxed with 1-bromo-undecane in CH_2Cl_2 for 12 h. After filtration, the solid was dissolved in 0.5 M NaOH and stirred for 15 min. Extraction with CH_2Cl_2 gave *N*-undecyl-dihydroindole. The dihydroindole was coupled with 5-nitrosalicylaldehyde and SiO_2 column chromatography afforded pure C11-nitroBIPS (Fig. 1*A*).

Plasmid Construction. Dronpa-actin was subcloned into the pCDNA vector (Invitrogen) between the XhoI and HindIII restriction sites. For the study of zebrafish, Dronpa-actin was subcloned into the pT2KXIGΔin vector between the SpeI and NotI restriction sites. For protein purification, Dronpa was subcloned into the pTrcHisC vector (Invitrogen) between the XhoI and HindIII restriction sites and transformed into JM109 *Escherichia coli* (Promega) by using the manufacturer's recommended protocol. The Dronpa protein was expressed and purified according to the handbook of Ni-NTA affinity chromatography (Qiagen). All constructs were verified by DNA sequencing.

Cell Culture and Transfection. NIH 3T3 (Mouse embryonic fibroblast cell line) cells were grown in DMEM (Invitrogen) supplemented with 10% fetal bovine serum (Invitrogen), 1% penicillin–streptomycin (Invitrogen), and 0.2% Fungizone Amphotericin B (Invitrogen) and transfected by using an ECM 830 electroporator (BTX) with a 7-ms pulse of 210 V. The cultures were kept at 37 °C in a humidified atmosphere with 5% CO_2. *Xenopus* spinal cord explants cultures were prepared as described by Gomez *et al.* (2, 3).

Cultured Neurons. Dissociated hippocampal cultures were prepared from P1 rats and transfected, as described previously (4). After 8 DIV, cells were transfected with 1.5 μg of DNA per 12-mm coverslip by using calcium phosphate. Live cultures were imaged after 11 DIV by using a Zeiss LSM 510/NLO META confocal microscope. A Spectra-Physics MaiTai HP laser was used for 2-photon activation, and a 488-nm argon laser was used for imaging. One-micron optical sections were collected with a pixel time of 1.6 μs. Achroplan IR 40×/0.80 W or Achroplan IR 63×/0.95 W dipping objectives were used.

Labeling of Intracellular Proteins with 8-Iodomethyl-NitroBIPS. Cells from 16- to 20-h-old *Xenopus* spinal cord explants plated on poly-D-lysine-coated coverslips were treated with a freshly prepared solution of 100 μM 8-iodomethyl-nitroBIPS (1) for 5 min. The thiol-reactive optical switch readily crosses the plasma membrane and labels cysteine-containing peptides and proteins. Some cells in the explant preparations contained yolk that exhibited a red fluorescence that provided a convenient autofluorescence signal for OLID imaging microscopy.

Imaging System and Optical Manipulation of MC-and *cis*-Dronpa Fluorescence in Cells. Three different microscope systems were used to image and manipulate nitroBIPS-labeled cells. (*i*) Images were collected on an Olympus FluoView500 confocal microscope using a 60×, N.A. = 1.45 oil immersion objective. UV light pulses from a 100-W Hg-arc lamp filtered through a 365 ± 25 bandpass filter were controlled with a time-varying shutter (Vincent Associates) to drive the SP to MC transition and was described in Gomez *et al.* (3). The duration of the 365-nm pulse was varied from 5 to 500 ms. Imaging of MC and concomitant conversion of the MC-excited state to SP was driven by using 543-nm laser scanning at a rate of ≈3 frames per second, whereas the emission was collected by using a 560-nm long-pass filter. The fastest laser scan speed used translated into a 2-μs pixel dwell time. A typical optical switching cycle was composed of a 100-ms pulse of 365-nm light during continuous scanning of the 543-nm laser. The use of a laser power consistent with live-cell imaging converted all MC in the image field to SP within 5 scans. Thus, an optical switch cycle composed of the complete interconversion of SP to MC and then MC to SP within an image field required ≈1∼10 s. Because the shutter controlling the 365-nm light source was not synchronized with the scanning of the 543-nm laser, the MC-fluorescence intensity was averaged in cases where the 365-nm pulse spanned two sequential 543-nm laser scans, and in cases where the 365-nm pulse was contained within a single scan, the MC-fluorescence from the previous image was used to generate the average. (*ii*), A Zeiss 510 META NLO on a AxioImager Zl stand with a Spectra-Physics MaiTai HP ti:sapphire laser was also used to image and manipulate NitroBIPS and Dronpa optical switches in living cells. Excitation of the SP state of NitroBIPS was achieved by using 720-nm (2-photon) excitation of the image field with the 63×/0.95 NA LWD water-immersion dipping objective. The MC-to-SP transition was driven by using 543-nm excitation of the image field and the concomitant MC-fluorescence was imaged by using a bandpass filter. The fastest scan speed of the 2-photon laser translated into a 1.6-μs pixel dwell time. (*iii*), A Bio-Rad Radiance 2100 MP Rainbow Confocal/Multiphoton System was used to image and manipulate Dronpa-actin optical switches in living cells. Excitation of Dronpa was achieved by using 35% 800-nm 2-photon excitation of the image field with PlanApo 60× oil objective. Imaging of Dronpa and concomitant conversion of the fluorescence state to no fluorescence state was driven by using 30% of the maximum power from a 488-nm laser scanning at a frame rate of 0.32 Hz, whereas the 500- to 530-nm emission was collected through a 500-nm long-pass filter (HQ500LP) and a 530-nm emission filter (HQ530SP).

Dronpa Imaging in Zebrafish. Single-cell *s1011t:GAL4* and *s1020t:GAL4* embryos (4) were injected with plasmid DNA for *UAS:Dronpa* or *UAS:Dronpa-actin* at 20 ng/μl, along with 50 ng/μl transposase mRNA and 0.04% phenol red. Zebrafish were raised at 28.5 °C in E3 medium and imaged at 5 dpf. Dronpa-positive fish were selected for fluorescence after activation of Dronpa by a 365-nm UV lamp. For live imaging, zebrafish larvae were mounted in 2% low-melting-point agarose (Invitrogen) and bathed in E3 medium containing 0.02% tricaine (Sigma) to prevent motion artifacts. Two-photon activation and confocal imaging of Dronpa was performed on a Zeiss 510 Axioplan META system using the LSM510 bleach function and a 63× objective. Dronpa was activated by 2-photon with a 780-nm laser set at 25–35% power. For neurons, activation was performed for 2 scans at 1.6 μs per pixel (1,024 × 1,024 pixels per image frame), and confocal images were acquired with a 488-nm laser at 17–24% power for 1.6 μs per pixel with an optical slice of 4.4 μm. For muscle cells, activation was performed for 2 scans at 2.5 μs per pixel (512 × 512 pixels per image frame), and confocal images were acquired with a 488-nm laser at 4% power for 2.5 μs per pixel with an optical slice of 2.5 μm. Two-photon

activation of Dronpa was followed by 5 confocal images and repeated 10 times for all images.

Lock-in Detection and Correlation Images. An internal reference intensity profile, reflecting the time-varying change in *cis*-Dronpa emission in response to the train of 800-nm and 488-nm scans is established from a selected pixel region having little background and greater signal of interest, which represents a structure with a high density of Dronpa-actin or one of the 0.35-μm latex beads covalently labeled with Dronpa that are added to the preparation. A cross-correlation between the intensity of any pixel in the image, as a function of time, and the reference signal is calculated to yield the correlation coefficient that is displayed on a pixel-by-pixel basis to construct a correlation image, which reveals correlation between the raw intensity and the modulated intensity profile over the switching cycles. Any negative values of the correlation coefficient represent noncorrelation with the reference waveform and are set to zero. In some situations, e.g., Fig. S2, the squared value of the correlation coefficient (within the range of 0–1) is displayed to highlight the structures exhibiting higher values of correlation over those with lower values of correlation.

Unlike the intensity image, the correlation image enables discrimination between the signal and the background by the value of the correlation coefficient, i.e., the signal of interest assumes high value of correlation, whereas the background assumes low value of correlation. In addition this unique feature of the correlation image allows for effective post-image processing such as histogram manipulation and multithreshold display that can further improve the image contrast. A more detailed description is beyond the scope of this study and will be published elsewhere.

1. Sakata T, Yan Y, Marriott G (2005) Family of site-selective molecular optical switches. *J Org Chem* 70:2009–2013.
2. Gomez T, Harrigan D, Henely J, Robles E (2003) Working with *Xenopus* spinal neurons in live cell culture. *Methods Cell Biol* 71:130–154.
3. Gomez T, Robles E (2003) Imaging calcium dynamics in developing neurons. *Methods Enzymol* 361:407–422.
4. Scott EK, *et al.* (2007) Targeting neural circuitry in zebrafish using GAL4 enhancer trapping. *Nat Methods* 4:323–326.

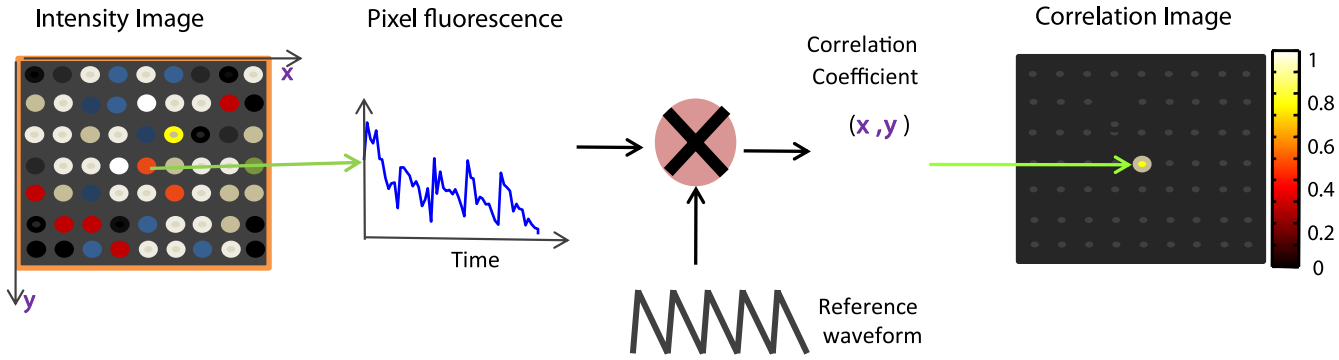

Fig. S1. Correlation imaging in OLID. To selectively amplify signals from the optical switch probes in the image field (*Left*), a cross-correlation analysis was performed between every pixel in an image field (*Left*) and a reference waveform (*Center*) to yield a correlation image (*Right*). Details are provided in *Results*.

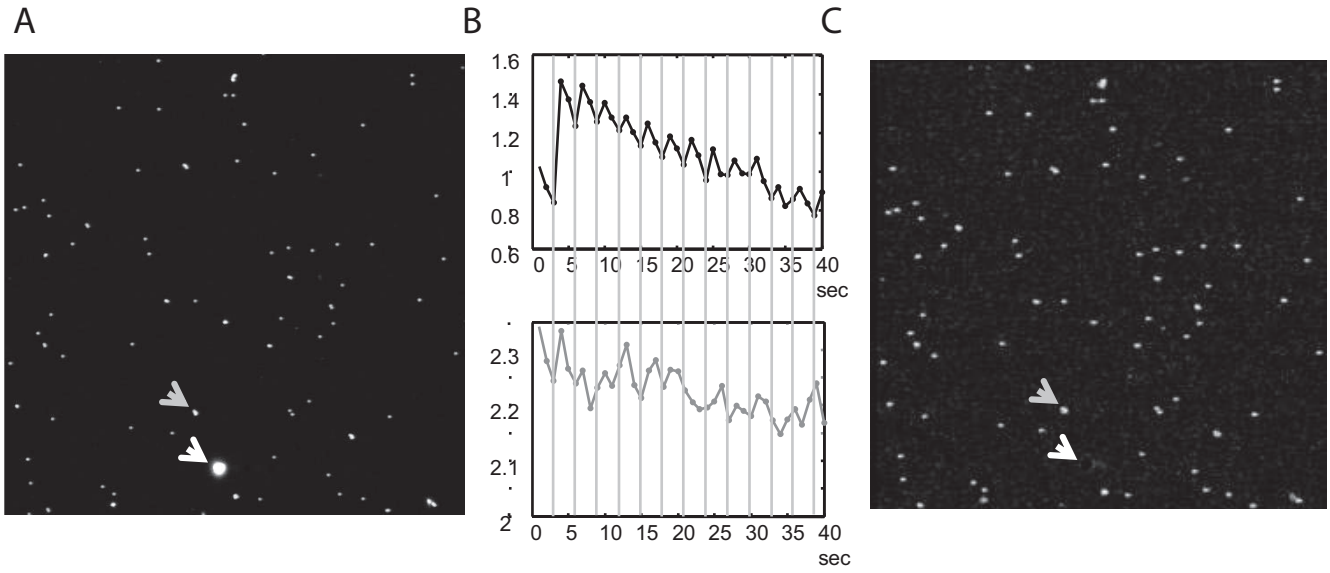

Fig. S2. OLID-enhanced images of beads bearing Dronpa in the presence of an aggregate of GFP-latex beads. (*A*) Image of fluorescence intensity from a mixture of ≈80 Dronpa-latex beads and a single larger aggregate of GFP-latex beads (white arrowhead). (*B*) (*Upper*) Black trace shows the fluorescence intensity profile (arbitrary units) of the reference waveform of the optical switching of a single Dronpa-latex bead (dark-gray arrowhead in *A*) according to the train of laser scans by using 800-nm 2-photon stimulation to convert nonfluorescent *trans*-Dronpa to the fluorescent *cis*-Dronpa and 488-nm stimulation to evoke fluorescence and the reverse isomerization, as shown. (*Lower*) Gray trace shows the fluorescence intensity (arbitrary units) profile within the larger aggregate of GFP-latex beads (white arrowhead in *A*). (*C*) Image of the square of the correlation coefficient of the beads from *A* derived from 12 cycles of optical switching. Note that all of the small Dronpa beads are visible, whereas the larger GFP bead (white arrowhead in *A*) is not.

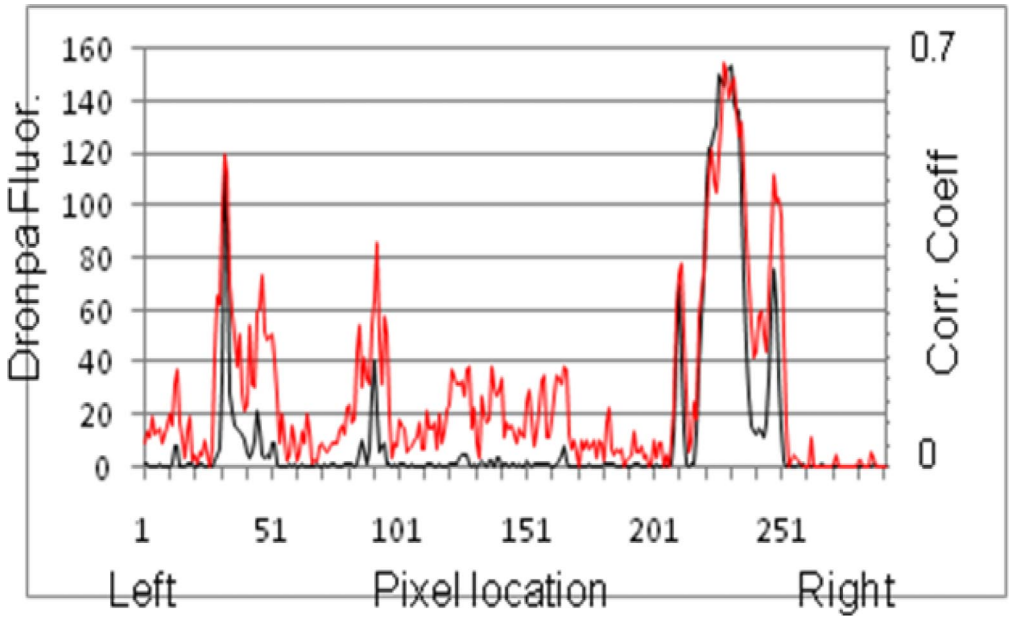

Fig. S3. Comparison of intensity and correlation images. Traces of Dronpa-actin fluorescence intensity (black, left axis) and the correlation coefficient (red, right axis) of Dronpa-actin in Fig. 4 *A* and *B* along the line defined by the yellow arrows in Fig. 4 *A* and *B*. Specific improvements to image contrast can be seen both visually (Fig. 4 *A* and *B*) and in the plot (above) for pixel loci from 40 to 200 that correspond to neuronal connections. Data were extracted by using ImageJ software and analyzed by using Excel.

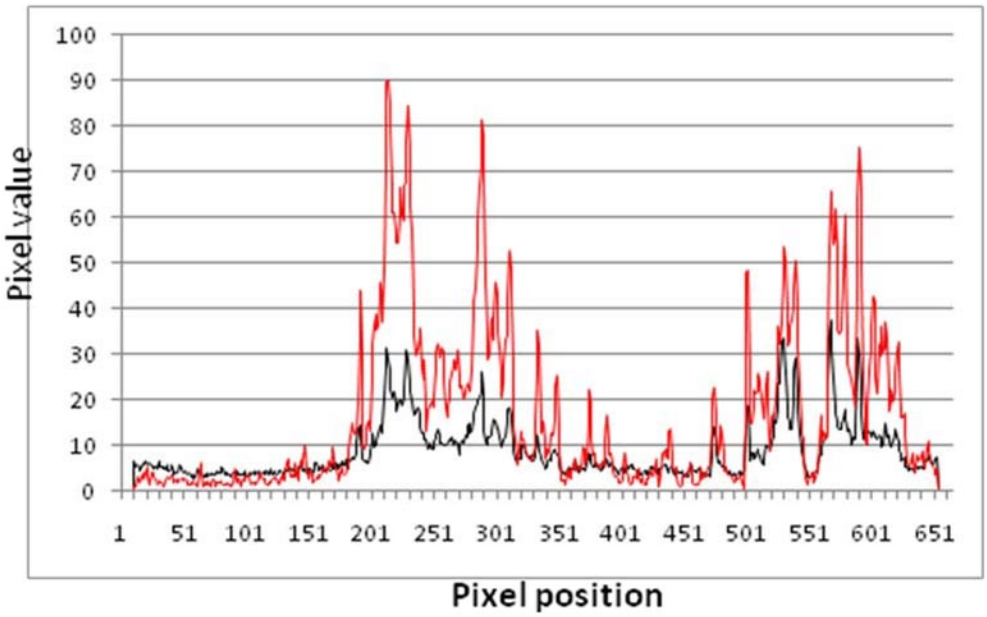

Fig. S4. Comparison of intensity and correlation images. Traces of the intensity (black, left scale) and correlation coefficient (red; scale is 0–1) of Dronpa along the line defined by the yellow arrows in Fig. 5 *D* and *E*. The signal-to-background for the intensity and correlation images were calculated for specific pixels along the trace shown in Fig. 5 *D* and *E*, choosing a region comprising only background and a Dronpa-labeled neuronal substructure. Data were extracted by using ImageJ software and analyzed by using Excel.